ELSEVIER

Journal of Structural Geology 27 (2005) 1061–1068

JOURNAL OF STRUCTURAL GEOLOGY

www.elsevier.com/locate/jsg

Coeval folding and boudinage in four dimensions

Janet Zulauf*, Gernold Zulauf

Department of Geology and Palaeontology, University of Frankfurt a.M., Senckenberganlage 32-34, D-60054 Frankfurt, Germany

Received 23 September 2004; received in revised form 25 March 2005; accepted 1 April 2005

Abstract

Scaled analogue experiments have been carried out incrementally to demonstrate the growth of constrictional folds and boudins through space and time. Pure constriction acted on a single stiff layer that was embedded in a weak matrix, with the layer trending parallel to the *X*-axis of the constrictional strain ellipsoid. The viscosity ratio between non-linear viscous layer and matrix was set at ca. 13. Three-dimensional images of the incrementally deformed layer have been obtained using computer tomography. They yielded clear evidence that D_1-folds and D_1-boudins show striking interactions when growing *simultaneously* at low to moderate finite strain. The axes of D_1-folds are subparallel and the axes of D_1-boudins are subperpendicular to the *X*-axis of the constrictional strain ellipsoid. The normalized wavelengths of D_1-folds and D_1-boudins, and the amplitudes of D_1-folds, are fixed already at low finite strain (-5%) and do not significantly change as deformation proceeds. The normalized wavelength of both structures is not so in line as suggested by theoretical studies. At higher degrees of finite strain, D_1-boudins are affected by D_2-folds, and rotated limbs of the latter show D_2-boudinage, resulting in complex deformation patterns that are difficult to identify in the field. The model results are important for the analysis and interpretation of deformation structures in rheologically stratified rocks undergoing dislocation creep under bulk constriction. Tectonic settings where constrictional folds and boudins may develop simultaneously are stems of salt diapirs, subduction zones or thermal plumes.

Keywords: Constriction; Analogue modelling; Diapir; Folding; Boudinage

1. Introduction

Buckle folds and boudins are common structures in rheologically stratified rocks and their geometry is widely used to constrain the kinematics, strain and rheology of natural tectonites (e.g. Ramberg, 1955; Sherwin and Chapple, 1968; Cobbold, 1976; Hudleston, 1973, 1986; Fletcher and Sherwin, 1978; Hudleston and Holst, 1984; Lacassin et al., 1993; Lan and Hudleston, 1996; Goscombe et al., 2004). In classical textbooks (e.g. Ramsay and Huber, 1987; Price and Cosgrove, 1990; Twiss and Moores, 1992; Gosh, 1993; Davis and Reynolds, 1996; Van der Pluijm and Marshak, 1997) buckle folds and boudins are largely treated as separate, 2D structures that result from plane-strain deformation of one or more stiff layers embedded in a weak matrix, with the layer oriented perpendicular to the *X*- and *Y*-axis of the finite strain ellipsoid, respectively. Consequently, folds and boudins should not develop simultaneously.

Results of theoretical studies (Ramberg, 1959, fig. 7; Ramsay, 1967; Talbot and Sokoutis, 1995; Weijermars, 1997, fig. 14.24) and analogue scale-model experiments (Kobberger and Zulauf, 1995; Zulauf et al., 2003), on the other hand, suggest that folds and boudins may grow during one single deformation event. This holds for all types of bulk coaxial deformation geometry (from pure flattening via plane strain to pure constriction), if particular geometrical and rheological boundary conditions are given. However, as the results of previous 3D-studies are based only on finite deformation structures, they cannot be used to prove if both structures grew simultaneously or in sequence.

The aim of the present work is to extend the earlier experimental studies of Kobberger and Zulauf (1995) and Zulauf et al. (2003). Different types of plasticine have been used for a stiff layer and a weaker matrix to model folding and boudinaging in rocks with power-law rheology. Layer and matrix underwent pure constriction, with the initially

* Corresponding author. Tel.: +49 69 79822108; fax: +49 069 79822958.
E-mail address: j.zulauf@em.uni-frankfurt.de (J. Zulauf).

0191-8141/$ - see front matter © 2005 Elsevier Ltd. All rights reserved.
doi:10.1016/j.jsg.2005.04.003

Table 1
Geometrical data of D_1-folds and D_1-boudins at 40% finite strain

	Run	I	II	III
	Number of deformation breaks	0	3	7
	ΔH (%)	11 ± 19	19 ± 13	0 ± 11
D_1-boudins	N	21 ± 3	17 ± 3	17 ± 4
	W_a (mm)	8.9	13.4	12.3
	W_d	5.0 ± 2.8	6.1 ± 3.4	6.5 ± 4.2
D_1-folds	N	4 ± 1	2 ± 1	2 ± 1
	W_a (mm)	17.0	16.9	29.7
	W_d	9.6 ± 3.0	9.9 ± 2.9	15.6 ± 4.7
	A (mm)	1.1 ± 0.6	0.8 ± 0.5	0.9 ± 0.5

A, amplitude of folds; ΔH, change in layer thickness; N, number of instabilities; W_a, dominant wavelength of instabilities; W_d, normalized dominant wavelength of instabilities.

planar layer oriented parallel to the X-axis of the finite strain ellipsoid. The deformation geometry of the layer has been analysed step by step using computer tomography (CT). A major advantage of this procedure is that the 3D-geometry of the developing 3D-deformation structures can be continually observed to finite amplitudes. It will be shown that (1) folds and boudins grow simultaneously during one and the same deformation event, (2) both structures do mutually interact, and (3) at least two generations of folds and boudins develop as deformation proceeds to higher finite strains. The results are important for the analysis and interpretation of deformation structures in rheologically stratified rocks undergoing dislocation creep under bulk constriction. Examples for constrictional tectonites are curtain folds in the stems of salt diapirs (Talbot and Jackson, 1987) and folds/boudins of subduction zones (Zulauf, 1997; Zulauf et al., 2002).

2. Methods, material and apparatus

The deformation apparatus used for the constrictional experiments consists of six aluminium plates which have been orthogonally assembled on top of a basal PVC plate. The movement of the plates allows pure constrictional strain to be performed (for further details on the machine, see Zulauf et al. (2003)). To reduce boundary effects due to friction between the specimen and the aluminium plates, the sides of the specimen were lubricated with vaseline. The initial model dimensions are $15 \times 15 \times 15$ cm. The analogue material consists of plasticine, a strain-rate softening material, the rheological parameters of which have been determined by previous investigations (for details concerning composition, rheological properties and supplier, see Zulauf and Zulauf (2004)). The experiments have been carried out at a temperature T of 25 °C with a viscosity contrast m of 13 between the stiff layer (Kolb brown plasticine) and the weak matrix (Beck's orange plasticine with 125 ml oil kg^{-1}). The apparent viscosity η and stress exponent n for the layer are 7.2×10^8 Pa s and 5.8, respectively, and for the matrix 6.1×10^7 Pa s and 7.0, respectively. These values are valid for a finite strain $e_{Y=Z}$ of 10% and a strain rate $\dot{e}$ of 6×10^{-5} s^{-1}. The matrix flows in steady state. The layer shows weak strain hardening (for further details, see Zulauf and Zulauf (2004)).

Three different experimental runs have been carried out to show the impact of stress relaxation due to deformation interruption. The first run was carried out without interruption. During the second and third runs, the deformation was stopped in each case at strain increments of 10 and 5%, respectively. The finite strain rate $\dot{e}$ was ca. 6×10^{-5} s^{-1}. Every experiment was finished at a finite strain of

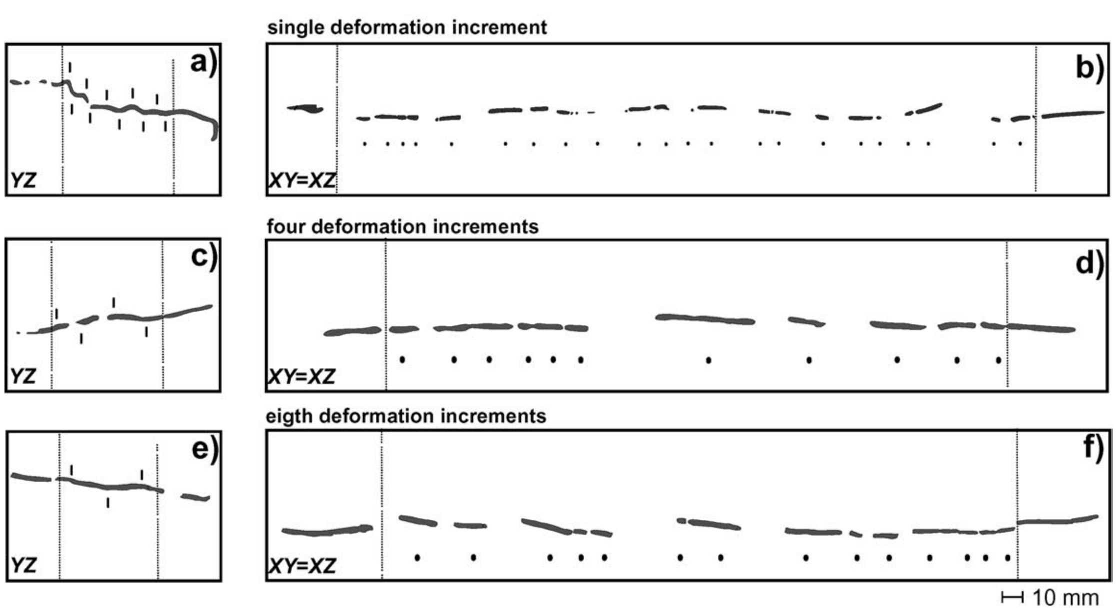

Fig. 1. Y- and $XY=XZ$-sections of different runs showing the geometry of the stiff layer after −40% finite strain. (a) and (b) Run 1 (single deformation increment); (c) and (d) Run 2 (four deformation increments); (e) and (f) Run 3 (eight deformation increments); vertical dashed lines indicate the boundaries of evaluated domain; point and dash indicate the number of structures (for further explanation, see text).